An example *Geophysics* article, with a two-line title

Joe Dellinger and Sergey Fomel†*

ABSTRACT

This is an example of using geophysics.cls for writing *Geophysics* papers.

INTRODUCTION

FWI is most efficient seismcic data inversion method due to its ability to use all the sesmic phasesin the seimic data. This involves the synthetic and observed data comparison in basis of the difference between them initial model is updated untill the synthetic data correspoing to the updated model satisfy the stopping criteria.
The amount of data involving in this method ehich is responsible for getting a better image is also a reason for enhancing the nonlinear relation between the data and physical parameters of the subsurface, it means the objective function prepared for the minimization is a multimodal function having a large number of minima and maxima as shown in FIGURE. this s responsible for FWI to stuck in local minima if the starting model is not lie within the basin of attraction. FWI is based on caluclas based optimization mehtods which have the tendency to move towards the nearest extrema this make it imposible to converge to global minima if starting model is in local basin of attraction. This make it neccesary to start the inversion with a inital model located near to the global minima.
Since the formulaisation of the FWI it have been gone through a long journey of developemnts to deal with challenges assiciated witht the nonlinearity such as multiscale focusing on low frequency data, normalized cros-corealtion obective function matching only the phases to mitigate the effect of amplitudes, and most recent optimal transport function to deal by increasing the convexity of the basin of attraction which increase the chance of falling the initial model in the basin of attraction of global minima.
This problem of stucking with the local minima is associated with the starting model. This problem can be dealt with preapring the initial model with the global optimization method becuase it have the ability to explore all the search space to find a optimal solution without the intervention of human being as required in ray based tomography metyhods for preapring the intial model by this it also reduce the chance of inclusion of human errors. this supermacy of global optimization motivated its utilization in prepasring the starting model for calculas based seismic inversion methods. The global optimization are inspired with the natural phenomina. the idea of preparing the initial model with the global optimization is because of the slow exploitation of

these methods. once the initial model is prepared with the confidence that it lie in the basin of global minima then local optimization statred with this model because local minima methods have high exploitation rate.
In geophysics, many authors proposed global optimization methods for geophysical data inversion such as Datta and Sen (2016) used the VFSA for preapring the initial model in this two step process parameterization of model is accomplished by the zero offset section, Fu et al. (2021) proposed a paralled VFSA algorithm for 1.5D acoustic FWI where model parameters are simultaneously updated across multiple threads.

The most commonly used global optimization methods in seismic data inversion are simulated annealing (SA) (refernce), genetic algorithm (GA) (reference), and particle swarm optimization (PSO) (references).
these methods are compared by Angleo Sajeva et al., 2017 to check the ability to deal the cases having large number of parameters
Y. Shiba and K. Irikura implemented the Very Fast Simulated Annealing (VFSA) algorithm to estimate earthquake displacement and demonstrated that VFSA outperforms the Genetic Algorithm (GA) in this task.
Rafael mendes et al. 2024, used a training image to guide the generation of realistic velocity model samples and enhance the convergence.
Datta et al., 2019 impliment the VFSA where the sedimentary layers and salt bodies are represnted by set of interfaces and ellipses respectively.
K Tran et al., 2012 used SA for inverting 2d shear wave velocity.
Alfredo Mazzotti et al., 2016 proposed GA FWI method involves parametrizing the subsurface with two grids: a coarse grid for inversion and a fine grid for modeling.
Malcolm Sambridge et al., 1992 compare the performance of GAs to Monte Carlo and find that GAs can achieve better fits with fewer model parameters and are computationally efficient.
Khiem T. Tran et al., 2012 demonstrates the potential of GA for improved characterization subsurface properties.
Chong Zeng wt al., 2011 studied GA for Rayleigh wave inversion
MattiaAleardi and Alferdo Mazzotti 2017 et al. proposed the seismic inversion with the GA with MCMC method to deal with the ucertainities in the search space.
Yang Haijun et al., 2017 developed a PSO based method for impedance inversion.
Ranjit Shaw et al., 2007 demonstrates the effectiveness of Particle Swarm Optimization (PSO) in inverting geophysical data for natural resource exploration.
K. Ding et al., 2015 focusing on the application of Particle Swarm Optimization (PSO) to solve geophysical inverse problems, specifically a 1D-DC resistivity case.
İsmail Kaplanvural et al., 2020 The research contributes to the literature by demonstrating the ability of PSO to invert common-offset GPR traces and estimate dielectric properties, including conductivity and relative magnetic permeability.
Juan Luis Fernández Martínez wt al. 2012 used PSO for reservoir characterization.
Juan Luis Fernández Martínez wt al. 2010 PSO algorithm's application to the SP inverse problem.

Ke Ding et al., 2015 compare the GA and PSO, conclude that PSO outperform the GA.

Oscar F. Mojica 2019 compare the GA and PSO, conclude that PSO outperform the GA.
Sajeva et al. (2017) presents a comparative analysis of four stochastic optimization methods—adaptive simulated annealing (ASA), genetic algorithm (GA), neighborhood algorithm (NA), and particle swarm optimization (PSO) for 1D elastic full-waveform inversion and residual static computation, to determine the suitability of each method for specific geophysical optimization problems.

ESTABLISHED METHODS
It is neccessary to use the parametriation to represent the model with limited number of parameters to reduce the complexity as well the computational time. we have implimented a parameterization strategy where a model can be defined with the depthof interface, reate of change of velocity between interface, and velocity of the interface. this reduce the number of paramters to multifolds to deal with the curse fo dimensionality associated with the number of parameters involved in the inversion.
YOUR METHOD WHY
WHAT NEW and ADVANTAGE
PAPER BRIEF

in this both are used together because both have advantages and disadvantages global is best in exploration and local is best in exploitation. PSO is easily parallelized. Some of the appealing facts of PSO are its convenience, simplicity and easiness of implementation requiring. The prominent features of PSO are its easy implementation, robustness to control parameters and computation efficiency compared with other existing heuristic algorithms such as genetic algorithm in a continuous problem.
method

METHODOLOGY

This approach involves two steps. First, a coarse velocity model is prepared using PSO by optimizing the depth, interface velocity, and the rate of change of velocity between interfaces. This model serves as an initial model for conventional gradient-based FWI in the second step.

Particle Swarm Optimization

Particle Swarm Optimization (PSO) is a stochastic method developed by James Kennedy and Russell Eberhart in 1995. Inspired by the social behavior of birds flocking to find food, they formulated a mathematical model to simulate this behavior. This model is widely applied to solve various optimization problems. They identified that the fundamental principle guiding birds' food-finding behavior is their ability to communicate with each other. Each bird in the process knows its current position ($\mathbf{x}_i(t)$) and best position ($\mathbf{p}_i(t)$), determined by evaluating the fitness using a

cost function. Additionally, each bird shares its best position with others, contributing to the collective knowledge of the flock's best position ($\mathbf{g}(t)$). Each bird's next movement is adjusted by its own best, the flock's best, and its current position. This iterative process continues at each step, ultimately converging towards a globally optimal position through the collaborative effort of all birds.This natural phenomenon is mathematically described by the velocity update equation 1 and the position update equation 2.

- $\mathbf{x}_i(t)$ be the position of particle i at iteration t.
- $\mathbf{v}_i(t)$ be the velocity of particle i at iteration t.
- $\mathbf{p}_i(t)$ be the personal best position of particle i until iteration t.
- $\mathbf{g}(t)$ be the global best position among all particles until iteration t.
- w be the inertia weight.
- c_1 and c_2 be the cognitive and social acceleration coefficients, respectively.
- r_1 and r_2 be random numbers uniformly distributed in the range $[0, 1]$.

The velocity and position update rules for each particle are given by:

$$\mathbf{v}_i(t+1) = w\mathbf{v}_i(t) + c_1 r_1(\mathbf{p}_i(t) - \mathbf{x}_i(t)) + c_2 r_2(\mathbf{g}(t) - \mathbf{x}_i(t)) \tag{1}$$

$$\mathbf{x}_i(t+1) = \mathbf{x}_i(t) + \mathbf{v}_i(t+1) \tag{2}$$

Where:

- w controls the influence of the previous velocity (inertia).
- c_1 and c_2 represent the trust of the particle in itself and in the swarm, respectively.
- r_1 and r_2 introduce stochasticity to the particle's movement.

Optimization Parameters

The updates in the Particle Swarm Optimization (PSO) algorithm are influenced by several controlling parameters, including the inertia weight (w), acceleration coefficients (c_1 and c_2), population size of the swarm, and the number of iterations. Among these, the inertia weight is the most critical tuning parameter as it balances the exploration and exploitation capabilities of PSO by adjusting the contribution of the

particle's previous velocity. An inertia weight value between 0.4 and 0.9 is generally found to provide good convergence. The cognitive and social coefficients (c_1 and c_2) represent the confidence in a particle's own best position and the swarm's best position, respectively, and they influence the updated velocity of the particles. The number of particles in the swarm also affects convergence; as the number of particles increases, the search space expands, potentially leading to better convergence. Experimental studies have shown that a swarm size of around 30 particles is generally effective for finding solutions within optimal iterations. The number of iterations, as with all iterative optimization algorithms, significantly impacts the performance of PSO.

This contribution of different parameters for succes of PSO make it is necessary to decide the combination of these parameters precisely. we have performed experiments to find the optimal combination of this values, for these experiment we have choose four nonlinear functions Ackley, Griewank, Rastrigin, and Styblinski-Tang function shown in figure **??**, **??**, **??**, and **??** respectively. These experiments are performed to determine the optimal value of the optimization coefficient and examine the relationship between the number of iterations and swarm size. Since both swarm size and iteration count impact computational time, it is essential to balance these factors to achieve effective optimization while minimizing computational costs. To fairly compare the effects of swarm size and the number of iterations, the rate of increase for both parameters is kept consistent. Following this, PSO is applied to the Schwefel function using the parameters chosen from the previous experiment to achieve the parameters that lead to the best convergence. To analyze performance, accuracy is evaluated based on the maximum deviation using equation 3. Further details of these experiments are outlined below.

$$Accuracy(\%) = 100 - \left| \frac{optimal\ value - evaluated\ value}{optimal\ value - maximum\ deviation} \right| \times 100 \qquad (3)$$

Where:

- *Optimal value*, best possible value of the objective function.
- *Evaluated value*, value of the objective function at a given point in the feasible domain.
- *Maximum deviation*, largest difference between the optimized value and the actual values.

1. Accuracy with Parameters: In this experiment, optimization is conducted for all specified test functions using varying values of c_1, c_2, and inertia weights, as illustrated in figures **??**, **??**, **??**, and **??**. To address the inherent randomness of this stochastic method, we perform 50 runs with 1000 iterations and calculate the average of these results as the final optimized values.

   This experiment concludes that a combination of inertia weights between 0.5 and 0.8, c_1 values ranging from 0.6 to 2.0, and c_2 values between 0.6 and 1.8 results in improved accuracy.

2. Accuracy with iterations: Here, accuracy is assessed while maintaining a constant swarm size of 30 and an initial iteration count of 1000, which is then increased by factors of 1.67, 2.0, 2.67, 3.00, 5, and 10, to examine how the number of iterations impacts accuracy across all test functions. The results indicate that as the number of iterations increases, accuracy improves, reaching a maximum close to 100 % when iterations are increased to 10 times, as illustrated in figure **??**.

3. Acuuracy with swarm size: In this study, accuracy is evaluated across all tests by varying the swarm size, starting with 30 particles and increasing it by factors of 1.67, 2.0, 2.67, 3.00, 5, and 10, while keeping the number of iterations constant at 1000. The findings indicate that as the swarm size increases, accuracy improves to approximately 70 %.

From these experiments for finding the optimization parameters, it is concluded that an optimal combination of inertia weights between 0.5 and 0.8, c_1 values ranging from 0.6 to 2.0, and c_2 values between 0.6 and 1.8 leads to enhanced accuracy. Additionally, increasing the number of iterations relative to the number of particles is beneficial, as it provide improved accuracy while maintaining similar computational costs.
The parameters that performed well in the previous experiments with test functions are used to evaluate the rate of convergence for the Schwefel function, as shown in figure **??**. This additional test function focuses solely on the objective function with respect to the number of iterations, as illustrated in figure **??**. The aim of this study is to identify a combination of optimization parameters that achieve a better rate of convergence, enabling optimized results to be obtained within fewer iterations. Figure **??** illustrates that higher values of inertia do not show convergence, while lower values of inertia exhibit a high rate of convergence but fail to reach the optimized value. An inertia value of 0.6 demonstrates good convergence with different c_1 and c_2 values. This analysis reveals that c_1 at 1.8 and c_2 at both 1.8 and 2.4 converge to zero, albeit slowly. In contrast, c_1 at 2.4 and c_2 ranging from 1.2 to 1.8 exhibit a good rate of convergence, reaching near zero within 100 iterations. Based on this analysis, the optimal parameters for further seismic inversion are set as inertia at 0.6, c_1 at 2.4, and c_2 between 1.2 and 1.8.

Model Parameterization

The seismic model includes physical parameters defined at densely packed grid points, often in the thousands, leading to an exponentially expanding search space that complicates the implementation of PSO. Therefore, it is essential to create a method for defining these velocity models with fewer parameters before implementing PSO, ensuring that the resulting output model can effectively serve as an initial model for FWI.
We propose a technique to define model with 1D depth-velocity profiles at sparse horizontal positions, as illustrated in Figure **??** with white vertical lines. This model

is representing a layered marine environment, where the velocity gradually increases with depth, ranging from 1500 to 4700 m/s. Additionally, it features a low-velocity layer situated between two high-velocity layers. The depth of interface in terms of grid point (d_i^k), where i represents the i^{th} interface for the k^{th} depth-velocity profile, (g_i^k) denotes the rate of change of velocity between the $(i-1)^{th}$ and i^{th} interfaces, and (v_i^k) indicates the velocity of the model at the i^{th} interface. These multiple, sparsely located depth-velocity profiles are interpolated using cubic splines to create an initial model. It is also assumed that no two interfaces intersect, as this is geologically implausible. Furthermore, the search space is restricted to feasible physical parameters. With these constraints, PSO is employed to optimize the three parameters for each layer in the development of the initial model.

PSO for Preparing Initial Model

The workflow of this implementation is illustrated in Figure **??**. It shows that initial model preparation begins with a uniform 1D depth-velocity profile as the initial model, where the velocity is same as upper layer and three parameters—depth, velocity at the interface, and the rate of change of velocity—are used as input parameters initially which are set to zero. A synthetic trace for this model is generated using an 8^{th}-order spatial scheme and a 2^{nd}-order temporal scheme. The synthetic trace is then compared to the observed data using the L2 norm, as described by equation 4. The observed data consists only near-offset data, where the major peaks are likely caused by reflectors directly beneath the shot location. The major peaks are selected from the observed data to guide the inversion process, with a focus on progressively inverting the reflectors defined by grid points. This approach falls into the category of over-parameterization as explained by (Sen Stoffa 1991), where the model is described by microlayers with thickness equal to the grid spacing. The inverted model justifying a particular peak used as an initial model for the next one. This process is repeated until the inversion successfully accounts for all the selected peaks for a shot. We allow flexibility in the timing of the selected peaks since it is not always precise to pinpoint the exact peak. The peaks resulting from multiples will not significantly impact the model because the interfaces causing these multiples have already been accounted. We sparsely select the shot locations and repeat this process for all chosen shots. Using the inverted reflectors from these shots, we create an initial model through interpolation and smoothing. This serves as the initial model for FWI.

$$O(syn^k, obs^k) = \sqrt{\sum_{i=1}^{N} (syn^k - obs^k)^2} \tag{4}$$

Where obs^k and syn^k indicate the observed data and synthetic data generated from the model, respectively; k refers to the shot number, and N represents the total samples.

Full Waveform Inversion

The model prepared using PSO serves as an initial model for FWI. Synthetic data is generated with this model and compared with the observed data, a process known as misfit calculation. Common methods for this calculation include the L2 norm, normalized cross-correlation function, Huber norm, and optimal transport function. The gradient of the objective function with respect to the model parameters is then calculated, which aids in updating the model. This iterative process ultimately leads to the recovery of velocity model.

THEORY

This is another section.

Equations

Section headings should be capitalized. Subsection headings should only have the first letter of the first word capitalized.

Here are examples of equations involving vectors and tensors:

$$\mathbf{R} = \begin{pmatrix} R_{\rm XX} & R_{\rm YX} \\ R_{\rm XY} & R_{\rm YY} \end{pmatrix} = \mathbf{P}_{M\to R}\,\mathbf{D}\,\mathbf{P}_{S\to M} \quad \mathbf{S} \quad , \tag{5}$$

and

$$R_{j,m}(\omega) = \sum_{n=1}^{N} \; P_j^{(n)}(\mathbf{x}_R)\; D^{(n)}(\omega)\; P_m^{(n)}(\mathbf{x}_S) \quad . \tag{6}$$

6 Note that the macro for the `\tensor` command has been changed to force tensors to be bold uppercase, in compliance with current SEG submission standards. This is so that documents typeset to the old standards will print out according to the new ones: e.g., tensor $\mathbf{T}$ (note converted to uppercase).

Figures

Figure 1 shows what it is about.

Multiplot

The first argument of the `multiplot` command specifies the number of plots per row.

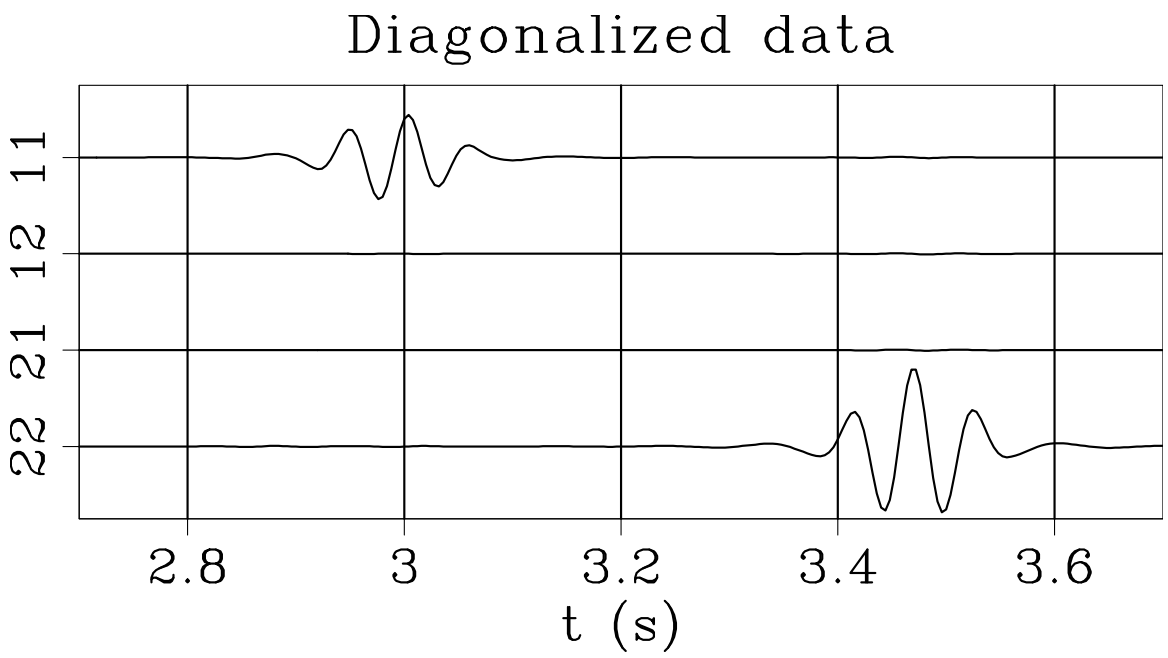

Figure 1: This figure is specified in the document by `\plot{waves}{width=\textwidth}{This caption.}`.

Tables

ACKNOWLEDGMENTS

I wish to thank Ivan Pšenčík and Frédéric Billette for having names with non-English letters in them. I wish to thank Červený (2000) for providing an example of how to make a bib file that includes an author whose name begins with a non-English character and Forgues (1996) for providing both an example of referencing a Ph.D. thesis and yet more non-English characters.

APPENDIX A

APPENDIX EXAMPLE

According to the new SEG standard, appendices come before references.

$$\frac{\partial U}{\partial z} = \left\{ \sqrt{\frac{1}{v^2} - \left[\frac{\partial t}{\partial g}\right]^2} + \sqrt{\frac{1}{v^2} - \left[\frac{\partial t}{\partial s}\right]^2} \right\} \frac{\partial U}{\partial t} \tag{A-1}$$

It is important to get equation A-1 right. See also Appendix B.

APPENDIX B

ANOTHER APPENDIX

$$\frac{\partial U}{\partial z} = \left\{ \sqrt{\frac{1}{v^2} - \left[\frac{\partial t}{\partial g}\right]^2} + \sqrt{\frac{1}{v^2} - \left[\frac{\partial t}{\partial s}\right]^2} \right\} \frac{\partial U}{\partial t} \tag{B-1}$$

Too lazy to type a different equation but note the numeration.

The error comparison is provided in Figure B-1.

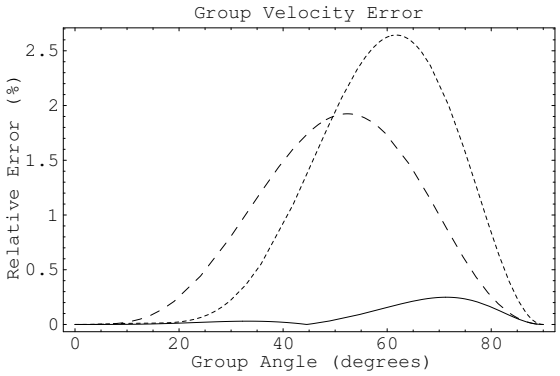

Figure B-1: This figure is specified in the document by `\sideplot{errgrp}{width=0.8\textwidth}{This caption.}`.

APPENDIX C

THE SOURCE OF THIS DOCUMENT

```
%\documentclass[paper]{geophysics}
\documentclass[paper,revised]{geophysics}
\usepackage{cleveref} %for cref

% An example of defining macros
\newcommand{\rs}[1]{\mathstrut\mbox{\scriptsize\rm #1}}
\newcommand{\rr}[1]{\mbox{\rm #1}}

\begin{document}

\title{An example \emph{Geophysics} article, \\ with a two-line title}

\renewcommand{\thefootnote}{\fnsymbol{footnote}}

\ms{GEO-Example} % paper number

\address{
\footnotemark[1]BP UTG, \\
```

```
200 Westlake Park Blvd, \\
Houston, TX, 77079 \\
\footnotemark[2]Bureau of Economic Geology, \\
John A. and Katherine G. Jackson School of Geosciences \\
The University of Texas at Austin \\
University Station, Box X \\
Austin, TX 78713-8924}
\author{Joe Dellinger\footnotemark[1] and Sergey Fomel\footnotemark[2]}

\footer{Example}
\lefthead{Dellinger \& Fomel}
\righthead{\emph{Geophysics} example}

\maketitle

\begin{abstract}
  This is an example of using \textsf{geophysics.cls} for writing
  \emph{Geophysics} papers.
\end{abstract}

\section{Introduction}

FWI is most efficient seismcic data inversion method due to its ability to use all th
\\
The amount of data involving in this method ehich is responsible for getting a better
\\
Since the formulaisation of the FWI it have been gone through a long journey of devel
\\
This problem of stucking with the local minima is associated with the starting model.
\\
In geophysics, many authors proposed global optimization methods for geophysical data

The most commonly used global optimization methods in seismic data inversion are simu
\\
these methods are compared by Angleo Sajeva et al., 2017 to check the ability to deal
\\
Y. Shiba and K. Irikura implemented the Very Fast Simulated Annealing (VFSA) algorith
\\
Rafael mendes et al. 2024, used a training image to guide the generation of realistic
\\
Datta et al., 2019 impliment the VFSA where the sedimentary layers and salt bodies ar
\\
K Tran et al., 2012 used SA for inverting 2d shear wave velocity.
\\
Alfredo Mazzotti et al., 2016 proposed GA FWI method involves parametrizing the subsu
```

```
\\
Malcolm Sambridge et al., 1992 compare the performance of GAs to Monte Carlo and  fin
\\
Khiem T. Tran et al., 2012 demonstrates the potential of GA  for improved characteriz
\\
Chong Zeng wt al., 2011 studied GA for Rayleigh wave inversion
\\
MattiaAleardi and Alferdo Mazzotti 2017 et al. proposed the seismic inversion with th
\\
Yang Haijun et al., 2017 developed a PSO based method for impedance inversion.
\\
Ranjit Shaw et al., 2007 demonstrates the effectiveness of Particle Swarm Optimizatio
\\
K. Ding et al., 2015 focusing on the application of Particle Swarm Optimization (PSO)
\\
İsmail Kaplanvural et al., 2020 The research contributes to the literature by demonst
\\
Juan Luis Fernández Martínez wt al. 2012 used PSO for reservoir characterization.
\\
Juan Luis Fernández Martínez wt al. 2010 PSO algorithm's application to the SP invers

Ke Ding et al., 2015  compare the GA and PSO, conclude that PSO outperform the GA.
\\
Oscar F. Mojica 2019 compare the GA and PSO, conclude that PSO outperform the GA.
\\
Sajeva et al. (2017) presents a comparative analysis of four stochastic optimization
\\

ESTABLISHED METHODS
\\
It is neccessary to use the parametriation to represent the model with limited number
YOUR METHOD WHY
\\
WHAT NEW and ADVANTAGE
\\
PAPER BRIEF



 in this both are used together because both have advantages and disadvantages global
Some of the appealing facts of PSO are its convenience, simplicity and easiness of im
The prominent features of PSO are its easy implementation, robustness to control para
method \ref{method}
\section{Methodology}
\label{method}
```

```
This approach involves two steps. First, a coarse velocity model is prepared using PS
\subsection{Particle Swarm Optimization}
Particle Swarm Optimization (PSO) is a stochastic method developed by James Kennedy a
\begin{itemize}
\item \( \mathbf{x}_i(t) \) be the position of particle \( i \) at iteration \( t \).
\item \( \mathbf{v}_i(t) \) be the velocity of particle \( i \) at iteration \( t \).
\item \( \mathbf{p}_i(t) \) be the personal best position of particle \( i \) until i
\item \( \mathbf{g}(t) \) be the global best position among all particles until itera
\item \( w \) be the inertia weight.
\item \( c_1 \) and \( c_2 \) be the cognitive and social acceleration coefficients,
\item \( r_1 \) and \( r_2 \) be random numbers uniformly distributed in the range \(
\end{itemize}

The velocity and position update rules for each particle are given by:
\begin{equation}
\mathbf{v}_i(t+1) = w \mathbf{v}_i(t) + c_1 r_1 (\mathbf{p}_i(t) - \mathbf{x}_i(t)) +

\label{eqn:pso_1}
\end{equation}

\begin{equation}
\mathbf{x}_i(t+1) = \mathbf{x}_i(t) + \mathbf{v}_i(t+1)
\label{eqn:pso_2}
\end{equation}

Where:
\begin{itemize}
\item \( w \) controls the influence of the previous velocity (inertia).
\item \( c_1 \) and \( c_2 \) represent the trust of the particle in itself and in th
\item \( r_1 \) and \( r_2 \) introduce stochasticity to the particle's movement.
\end{itemize}
\subsection{Optimization Parameters}
The updates in the Particle Swarm Optimization (PSO) algorithm are influenced by seve
\\
This contribution of different parameters for succes of PSO make it is necessary to d
\begin{equation}
Accuracy (\%) = 100 - \left| \frac{optimal \ value - evaluated \ value}{optimal \ val
\label{eqn:accuracy}
\end{equation}
Where:
\begin{itemize}
\item \(Optimal \  value\), best possible value of the objective function.
\item \(Evaluated \ value\), value of the objective function at a given point in the
\item \(Maximum \ deviation\), largest difference between the optimized value and the
\end{itemize}
```

```
\begin{enumerate}
\item Accuracy with Parameters: In this experiment, optimization is conducted for all
%\begin{figure}
% \includegraphics[width=\paperwidth]{Fig/ackley.png}
% \caption{Ackley function.}
% \label{fig:ackley}
%\end{figure}
%\begin{figure}
% \includegraphics[width=\paperwidth]{Fig/griewank.png}
% \caption{Griewank function.}
% \label{fig:griewank}
%\end{figure}
%\begin{figure}
% \includegraphics[width=\paperwidth]{Fig/rastrigin.png}
% \caption{Rastrigin function.}
% \label{fig:rastrigin}
%\end{figure}
%\begin{figure}
% \includegraphics[width=\paperwidth]{Fig/styblinski.png}
% \caption{Styblinski-Tang function.}
% \label{fig:styblinski}
%\end{figure}

This experiment concludes that a combination of inertia weights between 0.5 and 0.8,
% \begin{sidewaysfigure}
% \includegraphics[width=\paperwidth]{Fig/ackley_para_vs_accuracy.jpeg}
% \caption{Optimization of the Ackley function with varying inertia weights, \(c_1\),
% \label{fig:acc_ackley}
% \end{sidewaysfigure}
% \begin{sidewaysfigure}
% \includegraphics[width=\paperwidth]{Fig/griewank_para_vs_accuracy.jpeg}
% \caption{Optimization of the Griewank function with varying inertia weights, \(c_1\
% \label{fig:acc_griewank}
% \end{sidewaysfigure}
% \begin{sidewaysfigure}
% \includegraphics[width=\paperwidth]{Fig/rastrigin_para_vs_accuracy.jpeg}
% \caption{Optimization of the Rastrigin function with varying inertia weights, \(c_1
% \label{fig:acc_rastrigin}
% \end{sidewaysfigure}
% \begin{sidewaysfigure}
% \includegraphics[width=\paperwidth]{Fig/styblinski_para_vs_accuracy.jpeg}
% \caption{Optimization of the Styblinski-Tang function with varying inertia weights,
% \label{fig:acc_styblinski}
% \end{sidewaysfigure}
```

```
\item Accuracy with iterations: Here, accuracy is assessed while maintaining a consta
% \begin{figure}
% \includegraphics[width=0.8\paperwidth]{Fig/iteration_vs_accuracy.jpeg}
% \caption{Accuracy variation with iterations keeping the swarm size at 30 for all te
% \label{fig:acc_itr}
% \end{figure}

\item Acuuracy with swarm size: In this study, accuracy is evaluated across all tests
\end{enumerate}
From these experiments for finding the optimization parameters, it is concluded that
\\
The parameters that performed well in the previous experiments with test functions ar
%\begin{figure}
% \includegraphics[width=0.8\paperwidth]{Fig/schwefel.png}
% \caption{Schwefel function.}
% \label{fig:schwefel}
%\end{figure}

%\begin{figure}
% \includegraphics[width=0.8\paperwidth]{Fig/con_vs_itr.jpg}
% \caption{Objective function versus iteration for Schwefel function.}
% \label{fig:con_schwefel}
%\end{figure}

\subsection{Model Parameterization}
The seismic model includes physical parameters defined at densely packed grid points,
\\
We propose a technique to define model with 1D depth-velocity profiles at sparse hori

%\begin{figure}
% \includegraphics[width=0.8\paperwidth]{Fig/parameterization.jpg}
% \caption{layered model.}
% \label{fig:parameterization}
%\end{figure}

\subsection{PSO for Preparing Initial Model}
The workflow of this implementation is illustrated in Figure \ref{fig:work_flow}. It
We sparsely select the shot locations and repeat this process for all chosen shots. U

%\begin{figure}
% \includegraphics[width=0.5\paperwidth]{Fig/flow_chart.png}
% \caption{Work-flow.}
% \label{fig:work_flow}
%\end{figure}
```

```
\begin{equation}
O(syn^k, obs^k) = \sqrt{\sum_{i=1}^{N} \left( syn^k - obs^k \right)^2}
\label{eqn:l2norm}
\end{equation}

Where \(obs^k\) and \(syn^k\) indicate the observed data and synthetic data generated

\subsection{Full Waveform Inversion}
The model prepared using PSO serves as an initial model for FWI. Synthetic data is ge
\section*{Theory}

This is another section.

\subsection{Equations}

Section headings should be capitalized. Subsection headings should
only have the first letter of the first word capitalized.

Here are examples of equations involving vectors and tensors:
\begin{equation}
\tensor{R} =
\pmatrix{R_{\rs{XX}} & R_{\rs{YX}} \cr R_{\rs{XY}} & R_{\rs{YY}}}
=
\tensor{P}_{M\rightarrow R} \; \tensor{D} \; \tensor{P}_{S\rightarrow M}
\;\;\; \tensor{S} \ \ \ ,
\label{SVD}
\end{equation}
and
\begin{equation}
R_{j,m}(\omega) =
\sum_{n=1}^{N} \, \,
P_{j}^{(n)}(\mathbf{x}_R) \, \,
D^{(n)}(\omega) \, \,
P_{m}^{(n)}(\mathbf{x}_S) \ \ \ .
\label{SVDray}
\end{equation}
\ref{SVDray}
Note that the macro for the \verb#\tensor# command has been changed to
force tensors to be bold uppercase, in compliance with current SEG
submission standards. This is so that documents typeset to the old
standards will print out according to the new ones: e.g., tensor
$\tensor{t}$ (note converted to uppercase).

\subsection*{Figures}
\renewcommand{\figdir}{Fig} % figure directory
```

```
Figure~\ref{fig:waves} shows what it is about.

\plot{waves}{width=\textwidth}
{This figure is specified in the document by \texttt{
    $\backslash$plot\{waves\}\{width=$\backslash$textwidth\}\{This caption.\}}.
}

\subsubsection{Multiplot}


The first argument of the \texttt{multiplot} command specifies the
number of plots per row.

\subsection{Tables}


\begin{acknowledgments}
I wish to thank Ivan P\v{s}en\v{c}\'{\i}k and Fr\'ed\'eric Billette
for having names with non-English letters in them.  I wish to thank
\cite{Cerveny} for providing an example of how to make a bib file that
includes an author whose name begins with a non-English character and
\cite{forgues96} for providing both an example of referencing a Ph.D.
thesis and yet more non-English characters.
\end{acknowledgments}

\append{Appendix example}
\label{example}

According to the new SEG standard, appendices come before references.

\begin{equation}
\frac{\partial U}{\partial z} =
\left\{
  \sqrt{\frac{1}{v^2} - \left[\frac{\partial t}{\partial g}\right]^2} +
  \sqrt{\frac{1}{v^2} - \left[\frac{\partial t}{\partial s}\right]^2}
\right\}
\frac{\partial U}{\partial t}
\label{eqn:partial}
\end{equation}
It is important to get equation~\ref{eqn:partial} right. See also
Appendix~\ref{equations}.

\append[equations]{Another appendix}
```

```
\begin{equation}
\frac{\partial U}{\partial z} =
\left\{
  \sqrt{\frac{1}{v^2} - \left[\frac{\partial t}{\partial g}\right]^2} +
  \sqrt{\frac{1}{v^2} - \left[\frac{\partial t}{\partial s}\right]^2}
\right\}
\frac{\partial U}{\partial t}
\label{eqn:partial2}
\end{equation}
Too lazy to type a different equation but note the numeration.

The error comparison is provided in Figure~\ref{fig:errgrp}.

\sideplot{errgrp}{width=0.8\textwidth}
{This figure is specified in the document by \texttt{
    $\backslash$sideplot\{errgrp\}\{width=0.8$\backslash$text\-width\}\{This caption.
}

\append{The source of this document}

\verbatiminput{geophysics_paper.tex}

\append{The source of the bibliography}

\verbatiminput{geophysics_reference.bib}

\newpage

\bibliographystyle{seg}  % style file is seg.bst
\bibliography{geophysics_reference}

\end{document}
```

APPENDIX D

THE SOURCE OF THE BIBLIOGRAPHY

```
@Book{lamport,
  author =  {L[eslie] Lamport},
  title =   {{\LaTeX: A} Document Preparation System},
  publisher =   {Addison-Wesley},
  year =   1994
}
```

```
@Book{kopka,
  author =  {H[elmut] Kopka and P[atrick] W[] Daly},
  title =   {Guide to {\LaTeX}},
  publisher =   {Addison-Wesley},
  year =   2004
}

@preamble{"\newcommand{\SortNoop}[1]{}"}
@Book{Cerveny,
  author = {V[] {\SortNoop{Cerveny}}\v{C}erven\'{y}},
  title = {Seismic Ray Method},
  year = {2000},
  publisher = {Cambridge University Press}
}

@PHDTHESIS{forgues96,
  author = {E. Forgues},
  title  = {Inversion linearis\'ee multi-param\`etres via la th\'eorie des rais},
  school = {Institut Fran\c{c}ais du P\'etrole - University Paris VII},
  year   = {1996}
}


@article{Datta2016,
abstract = {Full-waveform inversion (FWI) has become a popular method to estimate ela
author = {Datta, Debanjan and Sen, Mrinal K.},
doi = {10.1190/GEO2015-0339.1},
file = {:C\:/Users/VIKAS/AppData/Local/Mendeley Ltd./Mendeley Desktop/Downloaded/Datt
issn = {19422156},
journal = {Geophysics},
mendeley-groups = {global_optimization},
number = {4},
pages = {R211--R223},
title = {{Estimating a starting model for full-waveform inversion using a global opti
volume = {81},
year = {2016}
}


@article{Fu2021,
author = {Fu, Xin and Innanen, Kristopher A and Project, Crewes},
file = {:C\:/Users/VIKAS/AppData/Local/Mendeley Ltd./Mendeley Desktop/Downloaded/Fu,
mendeley-groups = {global_optimization},
pages = {1--3},
title = {{A new parallel simulated annealing algorithm for 1 . 5D acoustic full-wavef
```

```
year = {2021}
}
```

REFERENCES

Červený, V., 2000, Seismic ray method: Cambridge University Press.

Datta, D., and M. K. Sen, 2016, Estimating a starting model for full-waveform inversion using a global optimization method: Geophysics, **81**, R211–R223.

Forgues, E., 1996, Inversion linearisée multi-paramètres via la théorie des rais: PhD thesis, Institut Français du Pétrole - University Paris VII.

Fu, X., K. A. Innanen, and C. Project, 2021, A new parallel simulated annealing algorithm for 1 . 5D acoustic full-waveform inversion: 1–3.